Letter | Editors' Suggestion

Ultrafast spin dynamics in the proximate quantum spin liquid $\alpha-RuCl_3$

Haochen Zhang [1,2], Subin Kim [2], Young-June Kim,[2] Hae-Young Kee,[2,3] and Luyi Yang [1,2,4,*]

[1]*State Key Laboratory of Low Dimensional Quantum Physics, Department of Physics, Tsinghua University, Beijing 100084, China*

[2]*Department of Physics, University of Toronto, Toronto, Ontario, Canada M5S 1A7*

[3]*Canadian Institute for Advanced Research, Quantum Materials Program, Toronto, Ontario, Canada M5G 1M1*

[4]*Frontier Science Center for Quantum Information, Beijing 100084, China*

(Received 25 November 2023; accepted 22 July 2024; published 21 August 2024)

$\alpha-RuCl_3$ is a Kitaev material suggested to be a proximate quantum spin liquid in a certain temperature and magnetic field range. Nonequilibrium measurements of transient dynamics have been proposed to detect fractionalized particles that emerge in the spin liquid and to possibly drive the system into novel photoinduced magnetic states that cannot be accessed by conventional equilibrium probes. Here we study ultrafast spin dynamics of photoinduced excitations in $\alpha-RuCl_3$ using pump-probe transient grating spectroscopy. In the real part of the complex transient reflection coefficient $\Delta r/r$, we observe evidence of long-range antiferromagnetic correlations near the Néel temperature. Most intriguingly, above the Néel temperature in the Kitaev paramagnetic phase, we reveal a photoexcitation component sensitive to the in-plane magnetic field in the imaginary part of $\Delta r/r$. This component exhibits two distinct lifetimes of about tens of picoseconds. This photoexcitation component may be connected to novel photoexcited states in the Kitaev quantum spin liquid, and its lifetimes likely reflect the dynamics of unconventional spin excitations in the Kitaev model.

DOI: 10.1103/PhysRevB.110.L081111

Introduction. Quantum spin liquids are an exotic state of matter characterized by strongly entangled spins without magnetic order [1–3]. Among the forefront candidates for realizing this state are Kitaev materials [4,5], such as Na_2IrO_3 (Ref. [6]), polytypes of Li_2IrO_3 (Refs. [7–10]), $H_3LiIr_2O_6$ (Ref. [11]), and especially $\alpha-RuCl_3$ (Ref. [12]) (hereafter $RuCl_3$).

In $RuCl_3$, the discoveries of half-integer quantized thermal Hall conductivity [13,14] and quantum oscillations of thermal conductivity [15] have generated great excitement for the possibility of fractional spin excitations. Critical evidence for unconventional spin excitations in $RuCl_3$ is also given by the broad spectroscopic continuum in neutron scattering [16], Raman scattering [17], and terahertz absorption [18] measurements. This continuum signifies the multiparticle excitations of fractional particles, which are distinct from the well-defined sharp peaks for magnon excitations. Although a breakdown of conventional magnons has been proposed to explain the continuum [19], the observed fermionic character [20,21] and its prominence below $T_H \sim 100$ K (Refs. [16–18,20,21]), where the Kitaev exchange dominates over other spin interactions, highlight its unique features.

To further identify these low-energy excitations, nonequilibrium measurements of transient dynamics have been proposed, leveraging their superior sensitivity to excitations across distinct energy scales [22–24]. A significant example is the tracking of photoinduced quasiparticle dynamics traversing the superconducting gap (∼1 meV) in cuprate and iron-based superconductors, using probe light in the near-infrared to visible spectrum [25–31]. Such observations are possible due to the spectral weight redistribution between the low-frequency Drude peak, associated with superconducting electrons, and the high-energy interband transitions during the breaking and reformation of Cooper pairs [25–33]. Moreover, the nonequilibrium spin dynamics of Kitaev magnets are attracting increasing attention due to the potential to drive the system into novel magnetic states through mechanisms like ultrafast (de)magnetization [34,35], carrier photodoping [36,37], Floquet engineering [38,39], and quench dynamics [22,40].

Despite their profound significance, experimental studies of nonequilibrium photoexcited states in Kitaev materials remain nascent [34,37,41–45]. Most ultrafast work has so far focused on the low temperature regime [34,37,41,42,45], where the long-range magnetic correlation obscures the influence of the Kitaev interaction on optical responses. In Na_2IrO_3, for instance, a change in transient optical dynamics across the Néel temperature highlights an abrupt increase in the binding energy of Hubbard excitons upon entering the magnetically ordered phase [41]. Direct detection of spin dynamics in spin liquids presents significant challenges. Therefore, clear-cut measurements should be performed at intermediate temperatures, where the system likely approximates a Kitaev paramagnet. Such measurements have the potential to reveal critical information, such as the lifetimes of fractional particles and their interaction with other elements in the system.

Here we directly probe the ultrafast dynamics of spin excitations in the Kitaev paramagnetic regime in $RuCl_3$ using heterodyne transient grating spectroscopy. We scrutinize the

*Contact author: luyi-yang@mail.tsinghua.edu.cn

transient change in the complex reflection coefficient across different temperature and in-plane magnetic field regimes to differentiate photoexcitations by their origins. Below the Néel temperature ($T_N \sim 7$ K), we observe photoexcitations tied to the long-range antiferromagnetic order, with the transient reflection coefficient showing a sharp transition at T_N and suppression under magnetic fields. Most strikingly, in the Kitaev paramagnetic temperature regime, we discover a photoinduced transient reflection component that undergoes substantial amplitude shifts under the magnetic field. Additionally, the amplitude of this component fades away with increasing temperature and vanishes around $T_H \sim 100$ K, the crossover temperature from the Kitaev paramagnetic phase to the conventional paramagnetic phase [46]. These observations suggest that this component is associated with unusual spin excitations in the proximate Kitaev spin liquid. This component has two lifetimes of ∼10 ps and ∼55 ps, hinting at the dynamics of exotic Kitaev spin excitations.

Phased-resolved transient reflectance. Heterodyne transient grating spectroscopy, a technique excelling in *phase-sensitive* ultrafast optical response [47], has been applied to study photoinduced nonequilibrium excitations in a variety of strongly correlated materials [41,48–50], as well as ambipolar transport and spin transport in semiconductors [51–56]. This method captures transient changes in the complex reflection coefficient Δr, composed of in-phase (Re) and out-of-phase (Im) components relative to the equilibrium reflection coefficient r. By inspecting them at relevant temperature and magnetic field regimes, we can distinguish Δr components from different origins. In contrast, only the in-phase component is measured in conventional pump-probe reflectivity experiments. Details of the experimental methods and the heterodyne transient grating spectroscopy are provided in the Supplemental Material (SM) [57].

To clearly illustrate $\Delta r/r$ responses of $RuCl_3$, we first show time traces of the Re and Im signals at three representative temperatures. The signals are noticeably different in three different temperature regimes: high [Fig. 1(c)], intermediate [Fig. 1(b)], and low [Fig. 1(a)].

In the high temperature regime (>100 K), the system is in the conventional paramagnetic phase. Figure 1(c) shows that both $\mathrm{Re}\{\Delta r/r\}$ and $\mathrm{Im}\{\Delta r/r\}$ undergo an initial rapid relaxation within less than 1 ps, followed by a slow decay of ∼ 100 ps at 120 K. This behavior is attributed to the cooling of photoexcited hot carriers and their recombination, termed "SP" for "single particle" [Fig. 1(f)]. The ultimate return to equilibrium, via thermal diffusion on a much longer timescale, is shown as offsets in the figure, denoted as "Th" for "thermal." Since both components are insensitive to temperature and external magnetic fields (see the SM [57]), they represent conventional excitations unrelated to the Kitaev model.

Below $T_H \sim 100$ K, the system enters the Kitaev paramagnetic phase, where short-range spin correlations become strongly entangled and exotic fractionalized spin excitations may emerge. At 40 K, $\mathrm{Re}\{\Delta r/r\}$ shown in Fig. 1(b) displays a similar rapid rise and slow decay pattern as seen at 120 K, indicating conventional excitations with minor temperature and magnetic field dependence (Figs. S4 and S6 in the SM [57]). Conversely, compared to 120 K, $\mathrm{Im}\{\Delta r/r\}$ at 40 K

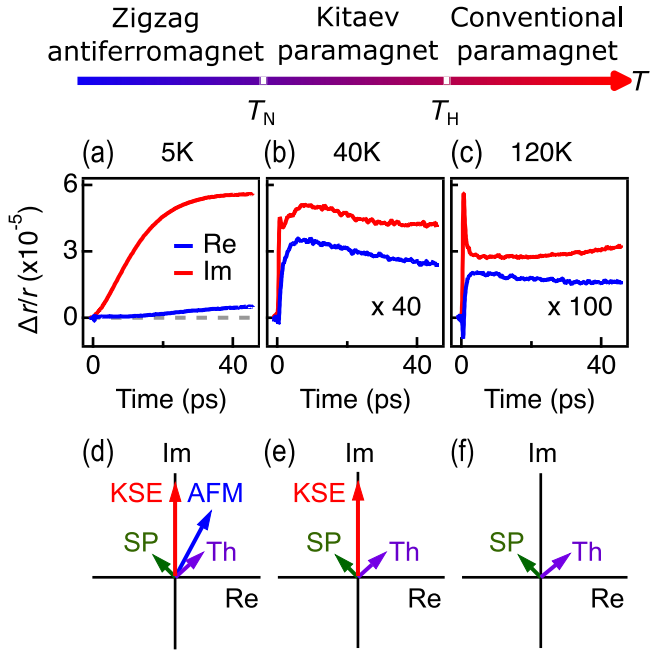

FIG. 1. Transient grating signals in $RuCl_3$ at three representative temperatures under zero magnetic field with a 190 nJ cm^{-2} laser fluence. (a)–(c) $\mathrm{Re}\{\Delta r/r\}$ and $\mathrm{Im}\{\Delta r/r\}$ at 5, 40, and 120 K, which are representative signals in the antiferromagnetic state, Kitaev paramagnetic state, and conventional paramagnetic state, respectively. The 40- and 120-K data are magnified by 40 and 100 times, respectively. (d)–(f) Schematics of the Δr phase diagrams in three different temperature regimes. Distinct Δr components represent different photoexcitation species. KSE: Kitaev spin excitations; AFM: AFM correlation; SP: single-particle excitations; Th: thermal diffusion process. The procedure to extract the optical phases is detailed in the SM [57].

exhibits distinct dynamics, with a component that rises and decays on ∼ 10 ps timescales after the initial rapid relaxation. This component in $\mathrm{Im}\{\Delta r/r\}$ has strong temperature and magnetic field dependence (discussed later), suggesting its association with the Kitaev spin excitations (KSEs). This KSE component may not be revealed in conventional pump-probe reflectivity that measures only $\mathrm{Re}\{\Delta r/r\}$ (see the SM [57]).

Below $T_N \sim 7$ K, a zigzag antiferromagnetic order appears, affecting both the in-phase and out-of-phase parts of $\Delta r/r$. Figure 1(a) reveals that the slow rise of $\mathrm{Re}\{\Delta r/r\}$ at 5 K differs from higher temperature trends and links to long-range magnetic correlations. Similarly, $\mathrm{Im}\{\Delta r/r\}$ at 5 K is characterized by slow dynamics, demonstrating that this antiferromagnetic component has projections on both the Re and Im axes.

Long-range magnetic order. We first investigate the effects of long-range magnetic correlations by examining the temperature and magnetic field dependence of $\Delta r/r$ near the Néel temperature.

Figures 2(a) and 3(a) present the Re and Im parts of $\Delta r/r$ versus time from 4.5 to 15 K, respectively, at a laser fluence of 38 nJ cm^{-2}. Influenced by the magnetic order, both parts have growing amplitudes with increasing temperature below T_N and exhibit amplitude jumps between 6.5 and 7 K. Crucially,

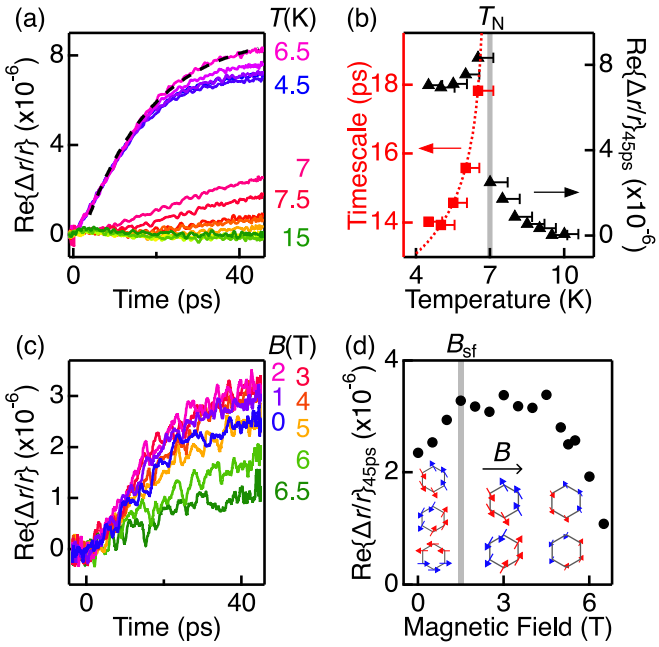

FIG. 2. Effects on $\mathrm{Re}\{\Delta r/r\}$ from the antiferromagnetic order. (a) $\mathrm{Re}\{\Delta r/r\}$ from 4.5 to 15 K under zero magnetic field with a pump fluence of 38 nJ cm^{-2}. The dashed line on the 6.5-K curve is a representative fit for the data below T_N using a single-exponential function with an offset. (b) The characteristic timescale obtained from fits to the data and the signal amplitude at 45 ps in (a) as a function of temperature. Error bars of the timescale are smaller than the markers. The dotted line is a power-law fit of the characteristic timescale showing the critical behavior near T_N. The markers represent the nominal temperatures measured by the thermometer, and the associated error bars for temperature, resulting from laser heating, were estimated by a model in Ref. [65], using the thermal conductivity data [66] and heat capacity data [67]. (c) $\mathrm{Re}\{\Delta r/r\}$ under an in-plane magnetic field from 0 to 6.5 T at 3.5 K with a pump fluence of 68 nJ cm^{-2}. The effective temperature is lower than T_N when laser heating is considered. (d) The signal amplitude at 45 ps in (c) as a function of the magnetic field. B_{sf} denotes the spin-flop transition, where the three zigzag antiferromagnetic domains transition into two.

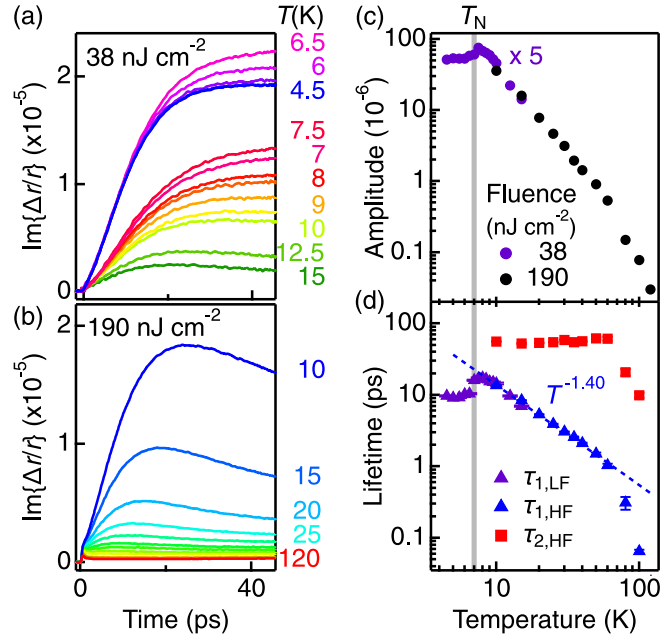

FIG. 3. Temperature dependence of $\mathrm{Im}\{\Delta r/r\}$. (a),(b) $\mathrm{Im}\{\Delta r/r\}$ from 4.5 to 15 K (38 nJ cm^{-2}) and from 10 to 120 K (190 nJ cm^{-2}). (c) Temperature dependent amplitude of KSEs. The low fluence data is multiplied by a factor of 5 to make up for the pump power difference. (d) Temperature dependence of the lifetimes of KSEs. τ_1 and τ_2 are the short and long lifetimes, respectively, with LF and HF indicating low (38 nJ cm^{-2}) and high (190 nJ cm^{-2}) fluence. Despite different pump fluences, the excellent overlap between the two data sets in (c) and (d) suggests that the amplitude scales linearly with the pump fluence and the lifetimes remain largerly fluence independent in the experiment's low power regime. The dotted line is the power-law fit to the data between 10 and 60 K. The temperature dependence of τ_1 yields a power-law exponent of -1.40 ± 0.05. Error bars in amplitude and lifetimes represent the χ^2 uncertainty when fitting the raw data in (a) and (b) to exponentials. Error bars in temperature are smaller than the markers.

$\mathrm{Re}\{\Delta r/r\}$ dies away around 10 K whereas $\mathrm{Im}\{\Delta r/r\}$ persists to higher temperatures, suggesting that KSEs reside in the Im part.

We focus on $\mathrm{Re}\{\Delta r/r\}$ to study the long-range magnetic correlation. After fitting the data below 7 K in Fig. 2(a) using a single exponential function with an offset, we plot the extracted characteristic timescale and the signal amplitude at 45 ps as a function of temperature in Fig. 2(b). Both the characteristic timescale and amplitude show divergent behavior as T_N is approached, signaling a connection to critical spin fluctuations near the ordering temperature [42,62–64]. In particular, the divergent spin fluctuations also manifest as an extremely slow-rising signal above T_N. Based on the amplitude of $\mathrm{Re}\{\Delta r/r\}$, we determine that the critical spin fluctuations preceding the magnetic ordering disappear around 15 K.

The enhancement of both the characteristic timescale and amplitude of the photoinduced reflectivity change has been observed in various systems undergoing second-order magnetic phase transitions [42,62–64,68]. In particular, the zigzag antiferromagnetic order was also probed in iridates by $\mathrm{Re}\{\Delta r/r\}$ with the standard pump-probe technique [42,43]. Due to the different specific heats of electron and spin reservoirs [69], the measured timescale reflects the relaxation time when the spin temperature reaches quasiequilibrium with the electron temperature [62].

$\mathrm{Re}\{\Delta r/r\}$ at low temperatures is also highly sensitive to the in-plane magnetic field, shown in Fig. 2(c), providing further evidence for its magnetic origin. Figure 2(d) illustrates that the amplitude of $\mathrm{Re}\{\Delta r/r\}$ at 3.5 K rises with an applied field up to ~ 1.5 T, then stabilizes on a plateau, and starts to decrease at ~ 4.5 T, continuing this decline until the maximum field of 6.5 T. The 1.5-T transition aligns well with the spin-flop transition identified by neutron scattering [70] and magneto-optical spectroscopy [71]. This transition corresponds to the rearrangement of the three zigzag antiferromagnetic domains into two, which preferentially align with the field direction. The amplitude drop at 4.5 T agrees with previous results on the decline of the magnetic order [70,71]. Notably, although an in-plane field of around 6 T can induce a transition into

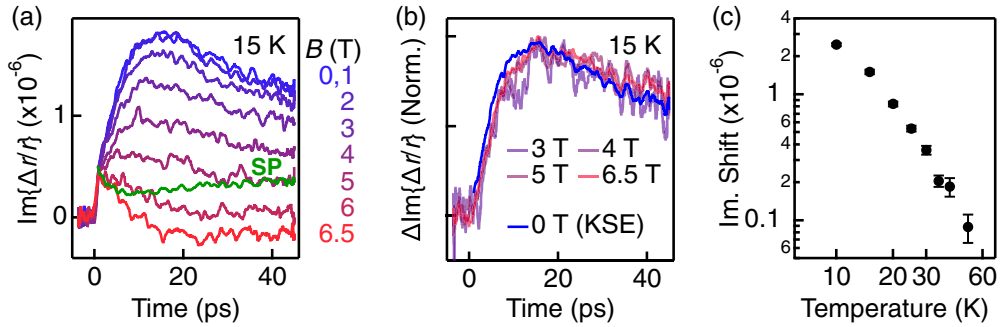

FIG. 4. Magnetic field dependence of $\mathrm{Im}\{\Delta r/r\}$. (a) $\mathrm{Im}\{\Delta r/r\}$ under the magnetic field from 0 to 6.5 T at 15 K. SP (the green curve): the contribution to $\mathrm{Im}\{\Delta r/r\}$ from the conventional single-particle excitations under the zero field that is inferred from the $\mathrm{Re}\{\Delta r/r\}$ signal after considering the SP component's optical phase [57]. (b) Shift of $\mathrm{Im}\{\Delta r/r\}$ (defined in main text) from 3 to 6.5 T at 15 K. The data below 3 T are not shown due to their small signal-to-noise ratio. All data are normalized. KSE stands for the Kitaev spin excitation component in $\mathrm{Im}\{\Delta r/r\}$. (c) $\mathrm{Im}\{\Delta r/r\}$ amplitude shift at 45 ps time delay as a function of temperature. Original time traces for other temperatures are shown in Fig. S7 in the SM [57]. The data were taken with a pump fluence of 517 nJ cm^{-2}.

an intermediate ordered phase due to interlayer exchange coupling (Refs. [71–73]), such a transition is not evident in our observations due to the limited field strength available.

Spin excitations in the Kitaev paramagnetic regime. As mentioned earlier, a distinct component in $\Delta r/r$ appears exclusively on the Im axis and below $T_{\mathrm{H}} \sim 100$ K. We now investigate this component in detail. Figures 3(a) and 3(b) provide the temperature dependence of $\mathrm{Im}\{\Delta r/r\}$ from 4.5 to 15 K at a pump fluence of 38 nJ cm^{-2}, and from 10 to 120 K at 190 nJ cm^{-2}, respectively. The higher fluence at intermediate temperatures is used to maintain acceptable signal quality. In Fig. 3(b), this component's thermal evolution can be clearly identified as a growing bump between 10 and 30 ps as temperature decreases.

To isolate the component relevant to the Kitaev paramagnetic temperature regime, we subtract the contributions of the long-range magnetic correlations and the single-particle excitations from $\mathrm{Im}\{\Delta r/r\}$ (see the SM [57]). The remaining signal in $\mathrm{Im}\{\Delta r/r\}$ can be fit with a double-exponential function, $A[\exp(-t/\tau_2) - \exp(-t/\tau_1)]$, with two lifetimes τ_1 and τ_2 where $\tau_1 < \tau_2$.

Figures 3(c) and 3(d) show the temperature-dependent amplitude and lifetimes of KSEs derived from the fits. Between 10 and 60 K, τ_1 exhibits a strong power-law dependence on temperature: $\tau_1 \propto T^{-1.40}$. By contrast, τ_2 (~55 ps) remains long-lived and largly unaffected by temperature change. Below 10 K, τ_1 decreases, likely owing to the development of magnetic order. Above 60 K, both the lifetimes and amplitude plummet with increasing temperature and disappear around 100 K due to the crossover from a Kitaev paramagnet to a conventional paramagnet. This is consistent with previous terahertz, inelastic neutron, and Raman scattering measurements [16–18,46,74].

In addition to the temperature dependence, the KSE component depends also strongly on the in-plane magnetic field. At 15 K, where long-range order is absent, applying a magnetic field significantly alters $\mathrm{Im}\{\Delta r/r\}$, as depicted in Fig. 4(a). The green curve is the conventional SP and thermal contributions to $\mathrm{Im}\{\Delta r/r\}$. The figure illustrates that the magnetic field modulates (rather than suppresses) the KSE's amplitude from positive to negative (compared to the green curve) as the field increases. Importantly, the shifts of $\mathrm{Im}\{\Delta r/r\}$ under different field values $[\Delta\mathrm{Im}\{\Delta r/r\}(B) \equiv \mathrm{Im}\{\Delta r/r\}(0\ \mathrm{T}) - \mathrm{Im}\{\Delta r/r\}(B)]$ can be scaled together and overlap well with the KSE component at zero field [15 K in Fig. 4(b), other temperatures in Fig. S8 in the SM [57]], demonstrating that the magnetic field does not affect the KSE component's lifetimes. Furthermore, the magnitude of the field-induced shift, calculated by $\Delta\mathrm{Im}\{\Delta r/r\}(6.5\ \mathrm{T})$ at 45 ps delay, decays with increasing temperature in a manner similar to the KSE's amplitude [Fig. 3(c)] and plummets at ~ 60 K. By contrast, the magnetic-field dependence of $\mathrm{Re}\{\Delta r/r\}$ is negligible in the same temperature regime (see Fig. S6 in the SM [57]).

The above analysis shows that the KSE component, emerging within the Kitaev paramagnetic temperature regime, is highly sensitive to in-plane magnetic fields. This confirms the origin of KSE from magnetic photoexcitations specific to this regime. This component likely probes the spin states within the energy continuum observed in neutron scattering [16], Raman scattering [17], and terahertz absorption [18] experiments. After the pump pulse excites electrons across the Hubbard gap, the relaxation of photoinduced carriers populates these low-energy spin states. We speculate that the transient optical response at the probe laser wavelength stems from the spectral weight transfer from the optical resonance at the Hubbard bands to these low-energy spin excitations. This mechanism is analogous to observations in ultrafast optical studies of cuprate and iron-based superconductors using near-infrared lasers [25–31,33]. However, it should be noted that while the superconducting condensate is described by a delta function at zero frequency, the continuum for fractional particles exhibits finite intensity and width. In superconductors, photoinduced conversion from a small fraction (1%) of the superconducting condensate to quasiparticles at the gap edge can cause a reflectance change of 10^{-4} at 1.55 eV (Refs. [30,75]), even if the superconducting gap is as small as 50 meV.

The two lifetimes revealed in our study could reflect the behaviors of fractional particles in the Kitaev model, specifically itinerant and localized Majorana fermion (MF) excitations [22]. Itinerant MFs likely show reduced lifetimes with

increasing temperature due to increased spin-phonon scattering, whereas localized MFs exhibit more thermally stable scattering rates. However, the observed $T^{1.40}$ decay rate diverges from the theoretical prediction of spin-phonon scattering rate, which anticipates a T^2 dependence [76]. We hope that our work will stimulate future theoretical exploration into the interplay among photoinduced charge, spin, and phonon excitations in realistic Kitaev materials.

Conclusions. In summary, we have studied the ultrafast spin dynamics in $RuCl_3$, a strong Kitaev spin liquid candidate, using optical transient grating spectroscopy. The observed changes in the complex transient reflection coefficient $\Delta r/r$ disclose distinct magnetic states in different temperature and magnetic field regimes. Near the Néel temperature, we have observed photoexcitations related to the long-range antiferromagnetic order in $\mathrm{Re}\{\Delta r/r\}$, which exhibits a sharp phase transition at the Néel temperature, and the signal amplitude is suppressed under high in-plane magnetic fields. In the Kitaev paramagnetic temperature regime, we have identified a component in $\mathrm{Im}\{\Delta r/r\}$ whose amplitude is sensitively tuned by the magnetic field and diminishes with increasing temperature. These results suggest links to photoinduced spin excitation in the proximate Kitaev spin liquid. This component has two distinct lifetimes of ∼10 ps and ∼55 ps, with the former exhibiting a $T^{-1.40}$ dependence and the latter being temperature insensitive. Our results provide direct evidence of spin dynamics inherent to the Kitaev spin liquid state and open the door for comprehensive studies on ultrafast nonequilibrium phenomena in Kitaev materials.

Acknowledgments. The work was supported by the National Natural Science Foundation of China (Grants No. 12074212 and No. 12361141826), the National Key R&D Program of China (Grants No. 2020YFA0308800 and No. 2021YFA1400100), the Beijing Natural Science Foundation (Grant No. Z240006), the Natural Sciences and Engineering Research Council of Canada (Grants No. RGPIN-2019-06449, No. RTI-2019-00809, and No. RGPIN-2022-04601), the Canadian Institute for Advanced Research, the Canada Foundation for Innovation, and the Ontario Research Fund. H.Z. was also supported by funds from the University of Toronto. H.-Y.K. acknowledges support from the Canada Research Chairs program.

[1] A. Kitaev, Anyons in an exactly solved model and beyond, Ann. Phys. **321**, 2 (2006).

[2] L. Balents, Spin liquids in frustrated magnets, Nature (London) **464**, 199 (2010).

[3] Y. Zhou, K. Kanoda, and T.-K. Ng, Quantum spin liquid states, Rev. Mod. Phys. **89**, 025003 (2017).

[4] H. Takagi, T. Takayama, G. Jackeli, G. Khaliullin, and S. E. Nagler, Concept and realization of kitaev quantum spin liquids, Nat. Rev. Phys. **1**, 264 (2019).

[5] S. Kim, B. Yuan, and Y.-J. Kim, $\alpha-RuCl_3$ and other kitaev materials, APL Mater. **10**, 080903 (2022).

[6] Y. Singh and P. Gegenwart, Antiferromagnetic mott insulating state in single crystals of the honeycomb lattice material Na_2IrO_3, Phys. Rev. B **82**, 064412 (2010).

[7] Y. Singh, S. Manni, J. Reuther, T. Berlijn, R. Thomale, W. Ku, S. Trebst, and P. Gegenwart, Relevance of the Heisenberg-Kitaev model for the honeycomb lattice iridates A_2IrO_3, Phys. Rev. Lett. **108**, 127203 (2012).

[8] K. A. Modic, T. E. Smidt, I. Kimchi, N. P. Breznay, A. Biffin, S. Choi, R. D. Johnson, R. Coldea, P. Watkins-Curry, G. T. McCandless *et al.*, Realization of a three-dimensional spin–anisotropic harmonic honeycomb iridate, Nat. Commun. **5**, 4203 (2014).

[9] T. Takayama, A. Kato, R. Dinnebier, J. Nuss, H. Kono, L. S. I. Veiga, G. Fabbris, D. Haskel, and H. Takagi, Hyperhoneycomb iridate $\beta-Li_2IrO_3$ as a platform for kitaev magnetism, Phys. Rev. Lett. **114**, 077202 (2015).

[10] F. Freund, S. C. Williams, R. D. Johnson, R. Coldea, P. Gegenwart, and A. Jesche, Single crystal growth from separated educts and its application to lithium transition-metal oxides, Sci. Rep. **6**, 35362 (2016).

[11] K. Kitagawa, T. Takayama, Y. Matsumoto, A. Kato, R. Takano, Y. Kishimoto, S. Bette, R. Dinnebier, G. Jackeli, and H. Takagi, A spin–orbital-entangled quantum liquid on a honeycomb lattice, Nature (London) **554**, 7692 (2018).

[12] K. W. Plumb, J. P. Clancy, L. J. Sandilands, V. V. Shankar, Y. F. Hu, K. S. Burch, H.-Y. Kee, and Y.-J. Kim, $\alpha-RuCl_3$: A spin-orbit assisted Mott insulator on a honeycomb lattice, Phys. Rev. B **90**, 041112(R) (2014).

[13] Y. Kasahara, T. Ohnishi, Y. Mizukami, O. Tanaka, S. Ma, K. Sugii, N. Kurita, H. Tanaka, J. Nasu, Y. Motome *et al.*, Majorana quantization and half-integer thermal quantum Hall effect in a kitaev spin liquid, Nature (London) **559**, 227 (2018).

[14] T. Yokoi, S. Ma, Y. Kasahara, S. Kasahara, T. Shibauchi, N. Kurita, H. Tanaka, J. Nasu, Y. Motome, C. Hickey *et al.*, Half-integer quantized anomalous thermal Hall effect in the kitaev material candidate $\alpha-RuCl_3$, Science **373**, 568 (2021).

[15] P. Czajka, T. Gao, M. Hirschberger, P. Lampen-Kelley, A. Banerjee, J. Yan, D. G. Mandrus, S. E. Nagler, and N. P. Ong, Oscillations of the thermal conductivity in the spin-liquid state of $\alpha-RuCl_3$, Nat. Phys. **17**, 8 (2021).

[16] A. Banerjee, J. Yan, J. Knolle, C. A. Bridges, M. B. Stone, M. D. Lumsden, D. G. Mandrus, D. A. Tennant, R. Moessner, and S. E. Nagler, Neutron scattering in the proximate quantum spin liquid $\alpha-RuCl_3$, Science **356**, 1055 (2017).

[17] L. J. Sandilands, Y. Tian, K. W. Plumb, Y.-J. Kim, and K. S. Burch, Scattering continuum and possible fractionalized excitations in $\alpha-RuCl_3$, Phys. Rev. Lett. **114**, 147201 (2015).

[18] Z. Wang, S. Reschke, D. Hüvonen, S.-H. Do, K.-Y. Choi, M. Gensch, U. Nagel, T. Rõõm, and A. Loidl, Magnetic excitations and continuum of a possibly field-induced quantum spin liquid in $\alpha-RuCl_3$, Phys. Rev. Lett. **119**, 227202 (2017).

[19] S. M. Winter, K. Riedl, P. A. Maksimov, A. L. Chernyshev, A. Honecker, and R. Valentí, Breakdown of magnons in a strongly spin-orbital coupled magnet, Nat. Commun. **8**, 1152 (2017).

[20] J. Nasu, J. Knolle, D. L. Kovrizhin, Y. Motome, and R. Moessner, Fermionic response from fractionalization in an insulating two-dimensional magnet, Nat. Phys **12**, 10 (2016).

[21] Y. Wang, G. B. Osterhoudt, Y. Tian, P. Lampen-Kelley, A. Banerjee, T. Goldstein, J. Yan, J. Knolle, H. Ji, R. J. Cava

et al., The range of non-kitaev terms and fractional particles in $\alpha-RuCl_3$, npj Quantum Mater. **5**, 14 (2020).

[22] J. Nasu and Y. Motome, Nonequilibrium majorana dynamics by quenching a magnetic field in kitaev spin liquids, Phys. Rev. Res. **1**, 033007 (2019).

[23] Y. Wan and N. P. Armitage, Resolving continua of fractional excitations by spinon echo in THz 2D coherent spectroscopy, Phys. Rev. Lett. **122**, 257401 (2019).

[24] W. Choi, K. H. Lee, and Y. B. Kim, Theory of two-dimensional nonlinear spectroscopy for the kitaev spin liquid, Phys. Rev. Lett. **124**, 117205 (2020).

[25] N. Gedik, M. Langner, J. Orenstein, S. Ono, Y. Abe, and Y. Ando, Abrupt transition in quasiparticle dynamics at optimal doping in a cuprate superconductor system, Phys. Rev. Lett. **95**, 117005 (2005).

[26] P. Kusar, V. V. Kabanov, J. Demsar, T. Mertelj, S. Sugai, and D. Mihailovic, Controlled vaporization of the superconducting condensate in cuprate superconductors by femtosecond photoexcitation, Phys. Rev. Lett. **101**, 227001 (2008).

[27] E. E. M. Chia, D. Talbayev, J.-X. Zhu, H. Q. Yuan, T. Park, J. D. Thompson, C. Panagopoulos, G. F. Chen, J. L. Luo, N. L. Wang, and A. J. Taylor, Ultrafast pump-probe study of phase separation and competing orders in the underdoped (Ba, K)Fe_2As_2 superconductor, Phys. Rev. Lett. **104**, 027003 (2010).

[28] Y. C. Tian, W. H. Zhang, F. S. Li, Y. L. Wu, Q. Wu, F. Sun, G. Y. Zhou, L. Wang, X. Ma, Q.-K. Xue *et al.*, Ultrafast dynamics evidence of high temperature superconductivity in single unit cell FeSe on $SrTiO_3$, Phys. Rev. Lett. **116**, 107001 (2016).

[29] J. P. Hinton, E. Thewalt, Z. Alpichshev, F. Mahmood, J. D. Koralek, M. K. Chan, M. J. Veit, C. J. Dorow, N. Barišić, A. F. Kemper *et al.*, The rate of quasiparticle recombination probes the onset of coherence in cuprate superconductors, Sci. Rep. **6**, 23610 (2016).

[30] I. M. Vishik, F. Mahmood, Z. Alpichshev, N. Gedik, J. Higgins, and R. L. Greene, Ultrafast dynamics in the presence of antiferromagnetic correlations in electron-doped cuprate $La_{2-x}Ce_xCuO_{4\pm\delta}$, Phys. Rev. B **95**, 115125 (2017).

[31] S. Wandel, F. Boschini, E. H. da Silva Neto, L. Shen, M. X. Na, S. Zohar, Y. Wang, S. B. Welch, M. H. Seaberg, J. D. Koralek *et al.*, Enhanced charge density wave coherence in a light-quenched, high-temperature superconductor, Science **376**, 860 (2022).

[32] H. J. A. Molegraaf, C. Presura, D. van der Marel, P. H. Kes, and M. Li, Superconductivity-induced transfer of in-plane spectral weight in $Bi_2Sr_2CaCu_2O_{8+\delta}$, Science **295**, 2239 (2002).

[33] C. Giannetti, F. Cilento, S. D. Conte, G. Coslovich, G. Ferrini, H. Molegraaf, M. Raichle, R. Liang, H. Eisaki, M. Greven *et al.*, Revealing the high-energy electronic excitations underlying the onset of high-temperature superconductivity in cuprates, Nat. Commun. **2**, 353 (2011).

[34] T. Amano, Y. Kawakami, H. Itoh, K. Konno, Y. Hasegawa, T. Aoyama, Y. Imai, K. Ohgushi, Y. Takeuchi, Y. Wakabayashi *et al.*, Light-induced magnetization driven by interorbital charge motion in the spin-orbit assisted Mott insulator $\alpha-RuCl_3$, Phys. Rev. Res. **4**, L032032 (2022).

[35] J. Zhang, N. Tancogne-Dejean, L. Xian, E. V. Boström, M. Claassen, D. M. Kennes, and A. Rubio, Ultrafast spin dynamics and photoinduced insulator-to-metal transition in $\alpha-RuCl_3$, Nano Lett. **23**, 8712 (2023).

[36] Y. Tian, W. Gao, E. A. Henriksen, J. R. Chelikowsky, and L. Yang, Optically driven magnetic phase transition of monolayer $RuCl_3$, Nano Lett. **19**, 7673 (2019).

[37] R. B. Versteeg, A. Chiocchetta, F. Sekiguchi, A. Sahasrabudhe, J. Wagner, A. I. R. Aldea, K. Budzinauskas, Z. Wang, V. Tsurkan, A. Loidl *et al.*, Nonequilibrium quasistationary spin disordered state in $\alpha-RuCl_3$, Phys. Rev. B **105**, 224428 (2022).

[38] S. A. Owerre, P. Mellado, and G. Baskaran, Photoinduced floquet topological magnons in kitaev magnets, Europhys. Lett. **126**, 27002 (2019).

[39] U. Kumar, S. Banerjee, and S.-Z. Lin, Floquet engineering of kitaev quantum magnets, Commun. Phys. **5**, 157 (2022).

[40] L. Rademaker, Quenching the kitaev honeycomb model, SciPost Phys. **7**, 071 (2019).

[41] Z. Alpichshev, F. Mahmood, G. Cao, and N. Gedik, Confinement-deconfinement transition as an indication of spin-liquid-type behavior in Na_2IrO_3, Phys. Rev. Lett. **114**, 017203 (2015).

[42] J. P. Hinton, S. Patankar, E. Thewalt, A. Ruiz, G. Lopez, N. Breznay, A. Vishwanath, J. Analytis, J. Orenstein, J. D. Koralek *et al.*, Photoexcited states of the harmonic honeycomb iridate $\gamma-Li_2IrO_3$, Phys. Rev. B **92**, 115154 (2015).

[43] N. Nembrini, S. Peli, F. Banfi, G. Ferrini, Y. Singh, P. Gegenwart, R. Comin, K. Foyevtsova, A. Damascelli, A. Avella, and C. Giannetti, Tracking local magnetic dynamics via high-energy charge excitations in a relativistic mott insulator, Phys. Rev. B **94**, 201119(R) (2016).

[44] D. Nevola, A. Bataller, A. Kumar, S. Sridhar, J. Frick, S. O'Donnell, H. Ade, P. A. Maggard, A. F. Kemper, K. Gundogdu *et al.*, Timescales of excited state relaxation in $\alpha-RuCl_3$ observed by time-resolved two-photon photoemission spectroscopy, Phys. Rev. B **103**, 245105 (2021).

[45] J. Wagner, A. Sahasrabudhe, R. Versteeg, Z. Wang, V. Tsurkan, A. Loidl, H. Hedayat, and P. H. M. van Loosdrecht, Nonequilibrium dynamics of $\alpha-RuCl_3$ – a time-resolved magneto-optical spectroscopy study, Faraday Discuss. **237** 237 (2022).

[46] S.-H. Do, S.-Y. Park, J. Yoshitake, J. Nasu, Y. Motome, Y. S. Kwon, D. T. Adroja, D. J. Voneshen, K. Kim, T.-H. Jang *et al.*, Majorana fermions in the kitaev quantum spin system $\alpha-RuCl_3$, Nat. Phys. **13**, 1079 (2017).

[47] N. Gedik and J. Orenstein, Absolute phase measurement in heterodyne detection of transient gratings, Opt. Lett. **29**, 2109 (2004).

[48] N. Gedik, J. Orenstein, R. Liang, D. A. Bonn, and W. N. Hardy, Diffusion of nonequilibrium quasi-particles in a cuprate superconductor, Science **300**, 1410 (2003).

[49] D. H. Torchinsky, F. Mahmood, A. T. Bollinger, I. Božović, and N. Gedik, Fluctuating charge-density waves in a cuprate superconductor, Nat. Mater. **12**, 387 (2013).

[50] J. P. Hinton, Quasiparticle coherence, collective modes, and competing order in cuprate superconductors (UC Berkeley, 2014), https://escholarship.org/uc/item/17f6q55b.

[51] C. P. Weber, N. Gedik, J. E. Moore, J. Orenstein, J. Stephens, and D. D. Awschalom, Observation of spin coulomb drag in a two-dimensional electron gas, Nature (London) **437**, 7063 (2005).

[52] L. Yang, J. D. Koralek, J. Orenstein, D. R. Tibbetts, J. L. Reno, and M. P. Lilly, Measurement of electron-hole friction in an n-Doped GaAs/AlGaAs quantum well using optical transient grating spectroscopy, Phys. Rev. Lett. **106**, 247401 (2011).

[53] L. Yang, J. D. Koralek, J. Orenstein, D. R. Tibbetts, J. L. Reno, and M. P. Lilly, Doppler velocimetry of spin propagation in a two-dimensional electron gas, Nat. Phys. **8**, 2 (2012).

[54] L. Yang, J. D. Koralek, J. Orenstein, D. R. Tibbetts, J. L. Reno, and M. P. Lilly, Coherent propagation of spin helices in a quantum-well confined electron gas, Phys. Rev. Lett. **109**, 246603 (2012).

[55] R. A. Duncan, G. Romano, M. Sledzinska, A. A. Maznev, J.-P. M. Péraud, O. Hellman, C. M. Sotomayor Torres, and K. A. Nelson, Thermal transport in nanoporous holey silicon membranes investigated with optically induced transient thermal gratings, J. Appl. Phys. **128**, 235106 (2020).

[56] J. Shin, G. A. Gamage, Z. Ding, K. Chen, F. Tian, X. Qian, J. Zhou, H. Lee, J. Zhou, L. Shi *et al.*, High ambipolar mobility in cubic boron arsenide, Science **377**, 437 (2022).

[57] See Supplemental Material at http://link.aps.org/supplemental/10.1103/PhysRevB.110.L081111 for details of (1) experimental methods, (2) heterodyne transient grating spectroscopy, (3) phase determination of the conventional pump-probe signals, (4) phase determination of the long-range magnetic order, (5) Kitaev spin excitations in $\mathrm{Im}\{\Delta r/r\}$, (6) negligible magnetic field dependence of $\mathrm{Re}\{\Delta r/r\}$ in the Kitaev paramagnetic regime, and (7) magnetic field dependence of $\mathrm{Im}\{\Delta r/r\}$ in the intermediate temperature regime, which also includes Refs. [5,47,50,58–61] therein.

[58] H. J. Eichler, P. Günter, and D. W. Pohl, *Laser-Induced Dynamic Gratings* (Springer-Verlag, Heidelberg, 1986).

[59] P. Voehringer and N. F. Scherer, Transient grating optical heterodyne detected impulsive stimulated raman scattering in simple liquids, J. Phys. Chem. **99**, 2684 (1995).

[60] A. A. Maznev, K. A. Nelson, and J. A. Rogers, Optical heterodyne detection of laser-induced gratings, Opt. Lett. **23**, 1319 (1998).

[61] G. D. Goodno, G. Dadusc, and R. J. D. Miller, Ultrafast heterodyne-detected transient-grating spectroscopy using diffractive optics, J. Opt. Soc. Am. B **15**, 1791 (1998).

[62] B. Koopmans, J. J. M. Ruigrok, F. D. Longa, and W. J. M. de Jonge, Unifying ultrafast magnetization dynamics, Phys. Rev. Lett. **95**, 267207 (2005).

[63] T. Ogasawara, K. Ohgushi, Y. Tomioka, K. S. Takahashi, H. Okamoto, M. Kawasaki, and Y. Tokura, General features of photoinduced spin dynamics in ferromagnetic and ferrimagnetic compounds, Phys. Rev. Lett. **94**, 087202 (2005).

[64] T. Kise, T. Ogasawara, M. Ashida, Y. Tomioka, Y. Tokura, and M. Kuwata-Gonokami, Ultrafast spin dynamics and critical behavior in half-metallic Ferromagnet: Sr_2FeMoO_6, Phys. Rev. Lett. **85**, 1986 (2000).

[65] Y. Xu, R. Wang, S. Ma, L. Zhou, Y. R. Shen, and C. Tian, Theoretical analysis and simulation of pulsed laser heating at interface, J. Appl. Phys. **123**, 025301 (2018).

[66] R. Hentrich, A. U. B. Wolter, X. Zotos, W. Brenig, D. Nowak, A. Isaeva, T. Doert, A. Banerjee, P. Lampen-Kelley, D. G. Mandrus *et al.*, Unusual phonon heat transport in $\alpha-RuCl_3$: strong spin-phonon scattering and field-induced spin gap, Phys. Rev. Lett. **120**, 117204 (2018).

[67] S. Widmann, V. Tsurkan, D. A. Prishchenko, V. G. Mazurenko, A. A. Tsirlin, and A. Loidl, Thermodynamic evidence of fractionalized excitations in $\alpha-RuCl_3$, Phys. Rev. B **99**, 094415 (2019).

[68] C. L. S. Kantner, M. C. Langner, W. Siemons, J. L. Blok, G. Koster, A. J. H. M. Rijnders, R. Ramesh, and J. Orenstein, Determination of the spin-flip time in ferromagnetic $SrRuO_3$ from time-resolved kerr measurements, Phys. Rev. B **83**, 134432 (2011).

[69] A. Kirilyuk, A. V. Kimel, and T. Rasing, Ultrafast optical manipulation of magnetic order, Rev. Mod. Phys. **82**, 2731 (2010).

[70] J. A. Sears, Y. Zhao, Z. Xu, J. W. Lynn, and Y.-J. Kim, Phase diagram of $\alpha-RuCl_3$ in an in-plane magnetic field, Phys. Rev. B **95**, 180411(R) (2017).

[71] J. Wagner, A. Sahasrabudhe, R. B. Versteeg, L. Wysocki, Z. Wang, V. Tsurkan, A. Loidl, D. I. Khomskii, H. Hedayat, and P. H. M. van Loosdrecht, Magneto-optical study of metamagnetic transitions in the antiferromagnetic phase of $\alpha-RuCl_3$, npj Quantum Mater. **7**, 28 (2022).

[72] C. Balz, L. Janssen, P. Lampen-Kelley, A. Banerjee, Y. H. Liu, J.-Q. Yan, D. G. Mandrus, M. Vojta, and S. E. Nagler, Field-induced intermediate ordered phase and anisotropic interlayer interactions in $\alpha-RuCl_3$, Phys. Rev. B **103**, 174417 (2021).

[73] C. Balz, P. Lampen-Kelley, A. Banerjee, J. Yan, Z. Lu, X. Hu, S. M. Yadav, Y. Takano, Y. Liu, D. A. Tennant *et al.*, Finite field regime for a quantum spin liquid in $\alpha-RuCl_3$, Phys. Rev. B **100**, 060405(R) (2019).

[74] A. Banerjee, C. A. Bridges, J.-Q. Yan, A. A. Aczel, L. Li, M. B. Stone, G. E. Granroth, M. D. Lumsden, Y. Yiu, J. Knolle *et al.*, Proximate kitaev quantum spin liquid behaviour in a honeycomb magnet, Nat. Mater. **15**, 733 (2016).

[75] G. P. Segré, Pump Probe Spectroscopy of Quasiparticle Dynamics in Cuprate Superconductors, Lawrence Berkeley National Laboratory, No. LBNL–47899, 787131, 2001, https://escholarship.org/uc/item/9wq894ph.

[76] K. Feng, M. Ye, and N. B. Perkins, Temperature evolution of the phonon dynamics in the kitaev spin liquid, Phys. Rev. B **103**, 214416 (2021).